Journal of
Ceramic Science
and Technology

J. Ceram. Sci. Tech., **02** [01] 39-46 (2011)
DOI: 10.4416/JCST2010-00030
available online at: http://www.ceramic-science.com
© 2011 Göller Verlag

Synthesis of PLLA-HA Hybrid Composites with Bone-Like Structure

J. Zhang*, D. Jiang, Z. Chen, Q. Lin and Z. Huang

The State Key Lab of High Performance Ceramics and Superfine Microstructure, Shanghai Institute of Ceramics, Chinese Academy of Sciences, Shanghai 200050, China

received July 02, 2010; received in revised form August 30, 2010; accepted September 23, 2010

Abstract

Many studies are currently underway to make synthetic bone-like materials with compositions of polymeric materials and hydroxyapatite (HA). In this paper, we report on the biomimetic preparation of poly-L-lactic acid (PLLA)/HA composites. Initially, HA nanorods with well-oriented organization were prepared with a simple hydrothermal method using dodecyl phosphate, a type of surfactant with a phosphorus head group, as the templating agent. The precipitate clusters consisting of hydroxyapatite nanorods exhibited a well-ordered microstructure. Subsequently, the obtained precipitates were dispersed in PLLA solutions to make slurries for tape casting. After homogenizing and tape casting, the obtained green sheets were further laminated and thermally compressed to form the final PLLA/HA composites. The microstructure and the resulting properties of the composites were investigated. The PLLA/HA composites containing nano-sized hydroxyapatite with structural features close to those of biological apatite make them attractive for bone tissue engineering applications.

Keywords: PLLA, HA, hybrid composites

I. Introduction

Natural bone is a composite material made up of a collagen fiber matrix stiffened by hydroxyapatite (HA) [1]. The collagen constitutes the main component of a three-dimensional matrix and manipulates the formation of apatite into a highly organized structure. This fine-tuning or adaptation of the structure to its function makes human bone a material with unique properties [2]. The generation of these organized nanostructured hybrid systems, using templates to guide the attachment, assembly of inorganic components from the nano-scale is an important challenge for the broad application of these materials.

To duplicate this high performance of natural bone, artificial bone materials have been produced in which organic substrates such as poly- (lactic acid), poly(L-lactide), peptide-amphiphile nanofibers, reconstituted collagen, chitosan, gelatinand inorganic substrate have been used in the mineralization [3, 4, 5, 6, 7, 8, 9, 10, 11, 12, 13, 14, 15, 16, 17].

Surfactants with hydrophilic and hydrophobic groups are often employed to direct organized superstructures owing to their specific self-assembly behavior in solutions [18]. Samuel I. Stupp *et al.* [19]designed self-assembling, synthetic substitutes for collagen, which can act as templates for hydroxyapatite crystallization. In the work of Clarkson *et al.* [20], the surfactant-docusate sodium salt was utilized to modify HA nanorods with a hydrophobic surface, and then these hydrophobic HA nanorods were organized into an enamel prism-like structure induced by solvent evaporation. Benson *et al*. used dodecylamine as the template and ordered hydroxyapatite (HA) nanorods were prepared after hydrothermal treatment [21]. Recently, Ye *et al*. prepared oriented HA using P123 and Tween 60 as the template [22].

Biodegradable poly-L-lactic acid (PLLA) is expected to be applicable as a material for the development of bone plates or for the temporary internal fixation of broken or damaged bones (for example see Ref. [23]). PLLA has also been used for drug delivery systems [24, 25]and in medicine as material for bone implants and bone fixation devices [26, 27, 28, 29, 30], surgical sutures [31, 32], and anastomotic devices [33]owing to their excellent biodegradation and biocompatibility.

The inclusion of HA into PLLA has been shown to increase the bone-cell responses *in vitro* and bone-forming ability *in vivo*, bone bonding ability (bioactivity) of the composite in comparison with natural polymers alone [34, 35]. Although the polymer composite with inorganic materials is well established, it is difficult to produce well-defined structures to increase their regenerative potential through the stimulation of protein mediation and cell adhesion and the subsequent matrix synthesis, because most biomaterials containing inorganic material are brittle and decomposable.

In this paper, we report on the biomimetic preparation of PLLA/HA composites. Initially, dodecyl phosphate, a type of surfactant with a phosphorus head group, was used as the templating agent to synthesize the oriented HA nanorods with a simple hydrothermal method. Subsequently, the nanorods were dispersed in PLLA solutions to make slurries for tape casting. Having been homogenized, the slurries were cast and the obtained green sheets were further laminated and pressed to form the final PLLA/HA composites. The microstructure and the

* Corresponding author: jxzhang@mail.sic.ac.cn

mechanical properties were investigated. The composites containing nano-sized hydroxyapatite with structural features close to those of biological apatite make them attractive for bone tissue engineering applications.

II. Experimental

(1) PLLA-HA composites

In the typical synthesis, calcium nitrate tetrahydrate ($Ca(NO_3)_2{\cdot}4H_2O$) and disodium hydrogen phosphate (Na_2HPO_4) were used as calcium and phosphorous sources for HA, respectively. Potassium lauryl phosphate (SUNMAP-K, Tian Jin Xian Guang Chemical Co. Ltd), which is a type of organic phosphorus surfactant, was used as the templating agent. The sample was prepared as follows: SUNMAP-K aqueous solution was prepared by adding SUNMAP-K to a fixed amount of water by stirring at 80 °C in a water bath. After being conditioned, the aqueous solution of Na_2HPO_4, $Ca(NO_3)_2{\cdot}4H_2O$ and NaOH was added separately and stirred into the surfactant solution. For these samples, the Ca: P_{total} molar ratio was kept at 1.67, where the P_{total} includes the P from the surfactant (P_{surf}) and from Na_2HPO_4. The Ca: P_{surf} molar ratio can be adjusted by adding different amounts of Na_2HPO_4. NaOH was used to adjust the solution pH between 10 and 12. The mixture was stirred at 80 °C in a water bath for 2 hours to yield a milky suspension. Then the suspension was transferred into an autoclave and treated in the temperature range of 120 - 160 °C for 24 hours (the hydrothermal pressure is in the range of 1.8 MPa – 2 MPa respectively). The resulting precipitates were washed three times with de-ionized water. After filtration, the gel-like paste was freeze-dried to yield white powder.

The green PLLA/HA sheets were prepared by dispersing HA powder in PLLA solutions (using dichloromethane as the solvent) to make slurries for tape casting. The content of HA is 0 wt%, 20 wt%, 50 wt%, 70 wt%, 80 wt% and 90 wt% respectively. After being homogenized, the slurries were tape-cast onto the Mylar sheets to obtain green sheets. The sheets were further laminated and pressed at 160 - 180 °C to form the final PLLA/HA composites. Pressing was performed in the pressure range of 10 - 15 MPa and held for 3 – 5 min.

(2) Characterization

Powder XRD patterns were obtained with a Rigaku D/MAX-2550V diffractometer. TEM analysis was performed using a JEOL 2100F electron microscope. The nano HA powder composition was determined with a Fourier transform infrared spectrometer in the 400 - 4000 cm^{-1} region. Microstructures of the samples were observed by field emission scanning electron microscopy (FESEM, JSM-6700F, JEOL, Tokyo, Japan).

Three-point bending strengths were measured with a universal testing machine (Instron 5565, Instron Corp, Canton, MA) at a crosshead speed of 0.1 mm/min and a span of 30 mm. The test pieces used were rectangular, $3 \times 4 \times 40$ mm^3 in size. Five pieces were tested for each composition.

(3) Biological test

The osteoblast-like cell line MG63 (Cells Resource Center of Shanghai Institute for Biological Science, Shanghai, China) was cultured at 37 °C in a humidified atmosphere of 5 % CO_2 in air, in 75-cm^2 flasks containing 10 ml of α-minimum essential medium (α-MEM), 10 % fetal calf serum, 2 mM L-glutamine, 1 % antimicrobial of penicillin, and streptomycin. After confluence, the cell monolayer was detached and re-suspended in the complete medium for reseeding onto the PLLA/HA sample surface.

Subsequently, the cell suspension with osteogenic medium was applied to sterilized, PLLA/HA disks (18 mm in diameter and 3 mm in thickness), which were placed into a 24-well culture plate. The culture plate was then transferred to an incubator, with the temperature being kept at 37 °C for 7 days. After each incubation time, the samples were taken out and rinsed with a phosphate-buffered saline solution and then fixed with glutaraldehyde solution in a sodium cacodylate buffer. Prior to SEM observation, the samples were dehydrated and dried in the hexamethyldisilizane ethanol solution series. Details of the cell culture process are well described in the literature [36].

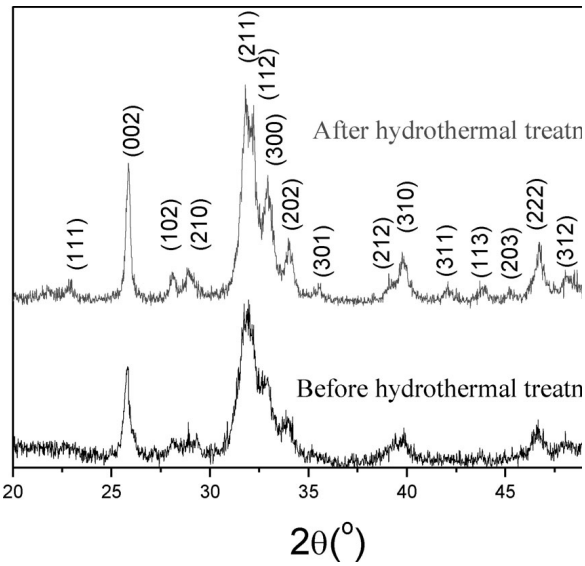

Fig. 1 : XRD patterns of HA before and after hydrothermal treatment.

III. Results and Discussion

(1) Precipitate characterization

The XRD pattern of HA powder before and after hydrothermal treatment is shown in Fig. 1. The XRD result revealed the characteristic peaks of pure HA, which was consistent with JCPDS files (9-432). Before hydrothermal treatment, the grain size and crystallinity degree were calculated to be 29.1 nm and 23.63 % respectively based on Scherrer's equation and reference [37]. This is in agreement with the extensive degree of peak broadening in the X-ray diffraction pattern shown in Fig. 1. After hydrothermal treatment, the grain size and crystallinity degree increased to 39.5 nm and 58.66 % respectively, in good agreement with the results shown in the literature [38]. As shown in Fig. 1, a preferred orientation in the [002] direction was observed in the sample series. The diffraction patterns suggest that the HA crystallites were aligned along the c-axes.

To obtain rod like HA grains, precipitation was conducted at 80 °C with a conditioning interval of 24 h. As shown in Fig. 2 (a), with only SUNMAP-K as the P source, a layered structure was observed with a periodical spacing of planes of 3.29 nm before hydrothermal treatment. This can be attributed to the surfactant templating structure. After the addition of Na_2HPO_4 as the P source, the layered structure disappeared (Fig. 2b). HA nanorods were found to form well-oriented aggregations, based on the alignment of each other along the c-axes. After hydrothermal treatment, the alignment of HA was well preserved, as shown in Fig. 2c. These assemblies appeared to be comprised of bundles of same-size nano-HA rods and aligned parallel to each other to yield an ordered matrix of island, suggesting that the building blocks of oriented attachment of nano-HA crystals are self-organized in order.

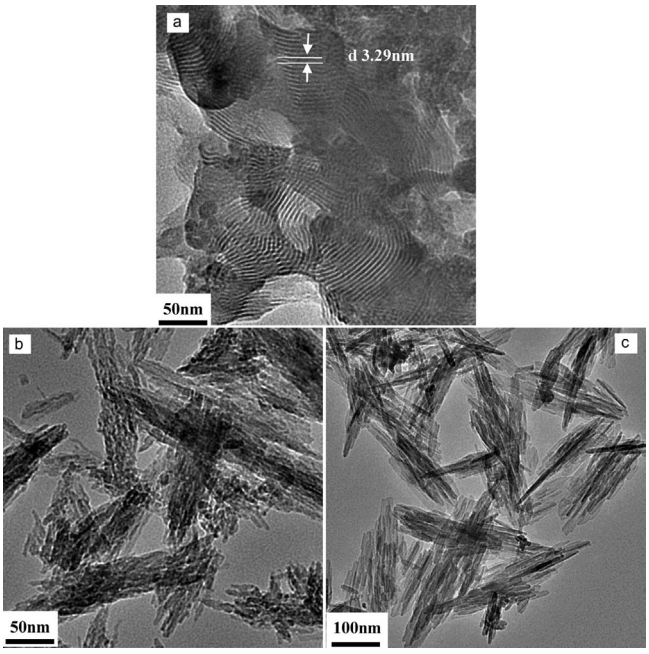

Fig. 2: TEM micrographs of HA before (a) (b) and after hydrothermal treatment (c).
(a) Without Na_2HPO_4 before hydrothermal treatment (with layered structure)
(b) With Na_2HPO_4/SUNMAP-K =2:1 before hydrothermal treatment (less ordered structure)
(c) After hydrothermal treatment at 160 °C of sample (b) (ordered structure)

As we know, phosphorus surfactants tend to self-assemble into a layered structure in water above the critical micelle concentration (CMC). After the Ca source was added (the Ca: P_{Surf} ratio was kept at 1.67), calcium phosphate phase tended to develop on the surface of the surfactant micelles as a result of the possible reaction between the Ca^{2+} ion and the phosphate head groups. TEM observation confirmed that a laminated microstructure was developed with alternating organic and inorganic layers (Fig. 2a). If more Ca^{2+} ions were added (with the corresponding addition of Na_2HPO_4 to keep the Ca:P_{total} ratio at 1.67), more calcium phosphate would be developed and the inorganic layer thickness would tend to increase. Although the effect of the surfactants is not strong enough to keep the mesoporous structure, it participates in the reaction and can effectively influence the arrangement of hydroxyapatite. Therefore, a less ordered layered structure will result. After hydrothermal treatment, HA nanorods tend to grow in preferred orientation and finally lead to the formation of a well-aligned structure. In this way, the final material consisting of well-oriented HA nanorods can be developed.

The HRTEM images (Fig. 3a) and selected area electron diffraction (SAED) pattern (Fig. 3b) indicate that all these synthetic nanorods are single crystals with a typical apatite crystalline structure. The crystal lattice planes were perfectly aligned and the lattice spacing was 0.346 nm, corresponding to the interplanar spacing of (002) planes for hexagonal HA. This reveals that the growth of HA occurs in the [002] direction. This is in agreement with the TEM observation and would suggest that the building blocks of oriented attachment of HA nanorods are self-organized into ordered structures similar to that observed in human bones.

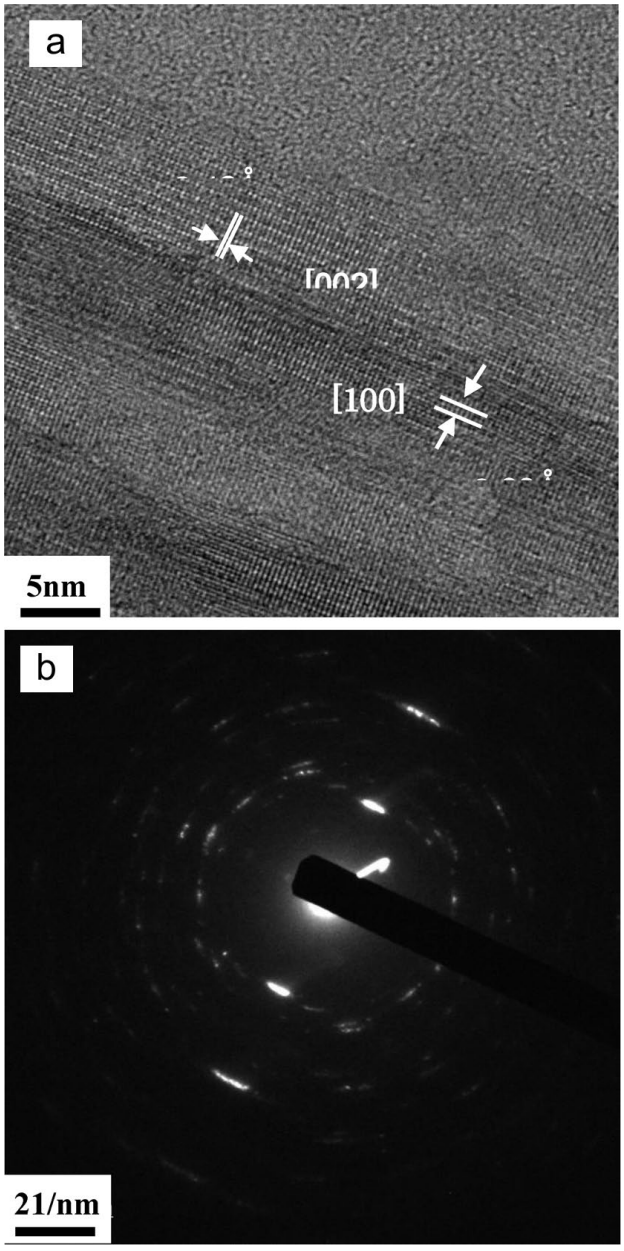

Fig. 3: HRTEM of HA composites after hydrothermal treatment.
(a) High resolution image showed the alignment of HA nanorods
(b) Electron diffraction showed the well-ordered structure

Fig. 4 shows the SEM micrographs of the samples. Bundles of nanorod-like HA crystals were observed in the samples, in agreement with the TEM observation. The EDS data show that the Ca/P ratio of these synthetic crystals is around 1.65, which approaches the theoretical ratio of HA (Ca/P = 1.67).

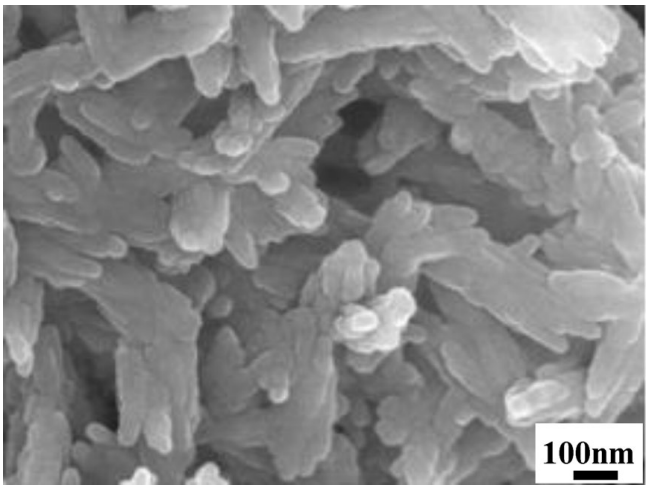

Fig. 4: Micrograph of HA composites after hydrothermal treatment. Bundles with well-aligned HA nanorods are shown.

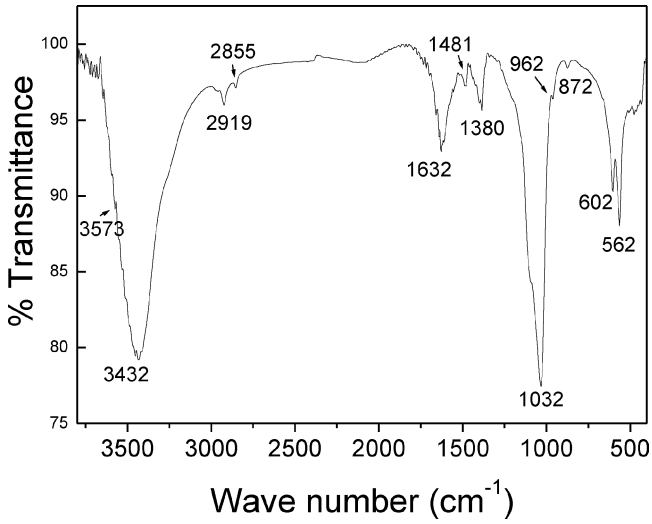

Fig. 5 : FTIR spectra of HA after hydrothermal treatment (the characteristic HA and the presence of SUNMAP-K peaks are shown).

The composition of the samples was characterized by FT-IR. From Fig. 5, we can see the existence of CH_2 peaks (2855 and 2919 cm^{-1}) and a CH peak (1632 cm^{-1}). This means that there are residual SUNMAP-K surfactants in the samples. The absorption band at 3570 cm^{-1} was assigned to the hydroxyl group in HA. It is not very sharp, which indicates that the OH^- group may have interactions with the organic surfactants. The band at 1032 cm^{-1} was assigned to the phosphate stretching vibration, while the bands at 602 and 562 cm^{-1} were due to the phosphate bending vibration. The characteristic peaks of PO_4^{3-} were found at 562, 602, 962 and 1032 cm^{-1}. Carbonate bands at 872, 1380 and 1481 cm^{-1} were also observed, which demonstrates that HA crystals prepared by the precipitation method contain carbonate ions in the structure. The carbonate might come from the atmosphere carbon dioxide during the whole reaction processes.

(2) Mechanical and biological properties

Fig. 6 shows SEM images of the microstructure of PLLA/HA composites at a weight ratio of 3 : 7. It was evident that these HA particles were uniformly distributed in the PLLA matrix. However, some agglomeration and void formation was observed in the composites containing larger volume fractions of HA. The phenomenon suggests that the interface between PLLA and HA phase has a close contact. These SEM micrographs confirmed that the selected solvent and synthetic technique should be an effective approach to prepare PLLA/HA composites that may be applied for biomedical engineering.

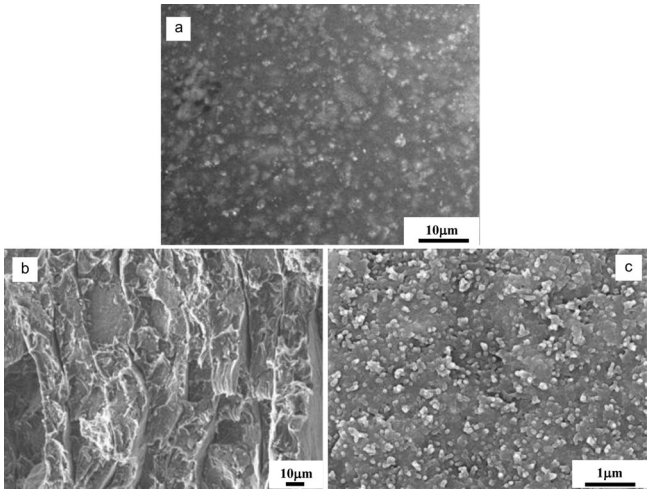

Fig. 6: Micrographs of PLLA/HA sheets and composites (with 70 wt% HA).
(a) PLLA/HA membrane with homogeneous distribution of HA
(b) Fracture surface of PLLA/HA showed layered structure
(c) High magnification of (b) showed the pullout of HA grains

Microscopy of the flexural fracture surfaces yielded interesting results. As shown in Fig. 6b, the fracture surface for PLLA/HA was relatively rough with an obvious layered structure and cracks visible along the interface between the layers. The HA grains in the foreground have been pulled out during the fracture; this might contribute to the high strength of the samples.

Fig. 7 shows the effect of the amount of HA in the composites on the failure strength and elastic modulus, respectively. There was an initial increase in strength at HA content lower than 50 wt% and a decrease thereafter. The PLLA/HA composites with high HA content (90 wt%) cannot be easily compacted and are not shown in Fig. 7. It has been reported that chemical bonding can occur between calcium phosphate particles and the PLLA matrix, with the attractions between oxygen ions in the PLLA ester group and the calcium ions in the calcium phosphate [39], these interactions may contribute to the increase in strength in HA-PLLA composites. However, these bonds between the particles and the matrix were not very strong. With higher loading of HA, the cross-sectional area of the load-bearing polymer is decreased and so the strength would be expected to decrease. Additionally, debonding of the matrix from the particles results in void formation, which lowers the tensile strength since cracks can more easily propagate through regions containing voids than through regions with filler content.

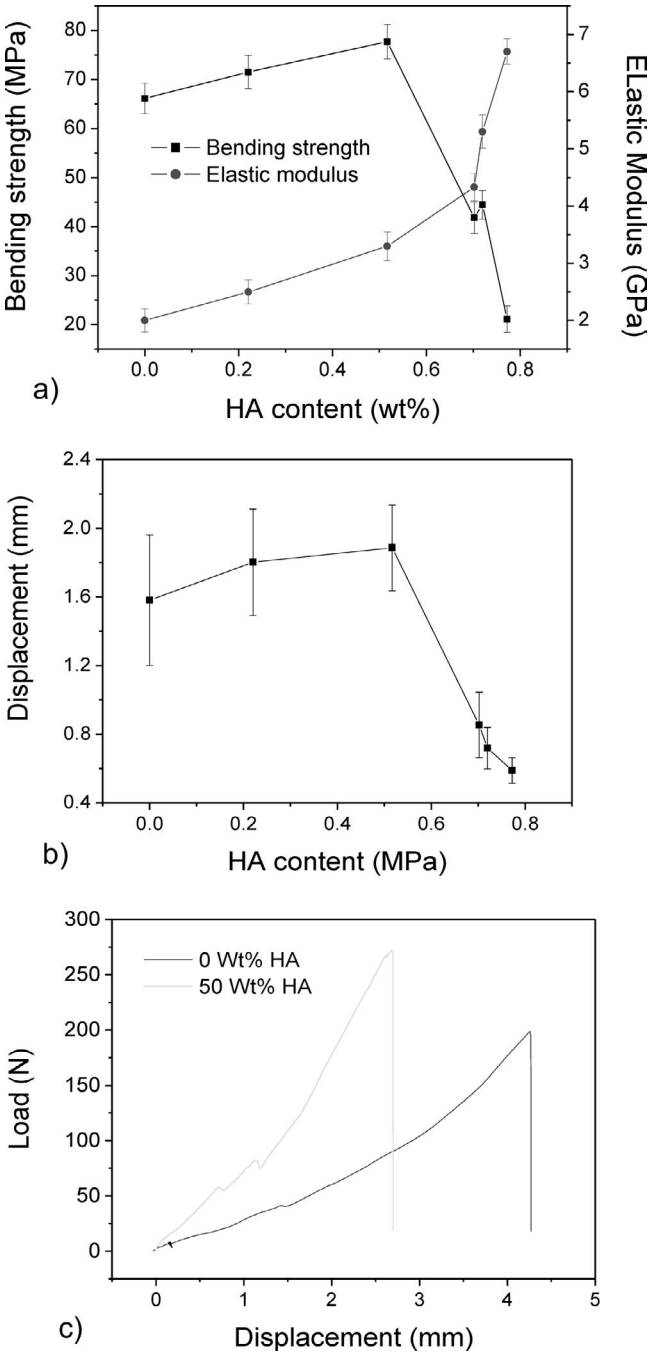

Fig. 7: Mechanical properties of PLLA/HA composites.
(a) Bending strength and elastic modulus.
(b) Displacement.
(c) Load-displacement curves.

The modulus of each material was significantly dependent on the HA content. Increasing the ceramic content would increase the modulus of the materials, with PLLA having the lowest modulus. The strain-to-failure curve was similar to that for the bending strength. At high HA content (> 50 wt%), there is a gradual decrease in strain to failure as more HA is added to the composite. In the composites, all the elongation arises from the polymer, since HA is rigid relative to the PLLA and tends to make the nanofiber matrix stiffer and less plastic in deformation, which is the typical characteristic of hard inorganic phase. Increasing the amount of filler may decrease the amount of polymer available for elongation and reduce the displacement. As shown in Fig. 7c, the PLLA-HA composites exhibit a characteristic failure behavior other than a linear one as observed in brittle materials. At higher PLLA content (> 20 wt%), the HA particles may be separated by continuous PLLA phase, though the strong bond was maintained between the HA particles and the PLLA molecules, the PLLA/HA samples became "soft" and as a result, no linear fracture mode resulted.

To assess the cellular response, the osteoblast-like cell line MG63 was cultured on the PLLA/HA samples (Fig. 8). After seeding for 3 days, the cells appear to be flat and are in close contact with the PLLA/HA composites (Fig. 8a). After seeding for 7 days, the cells become more elongated and thicker (Fig. 8b), indicating that the MG63 cells can attach and adhere well to the PLLA/HA substrate. Further work concerning *in vivo* biological tests is underway.

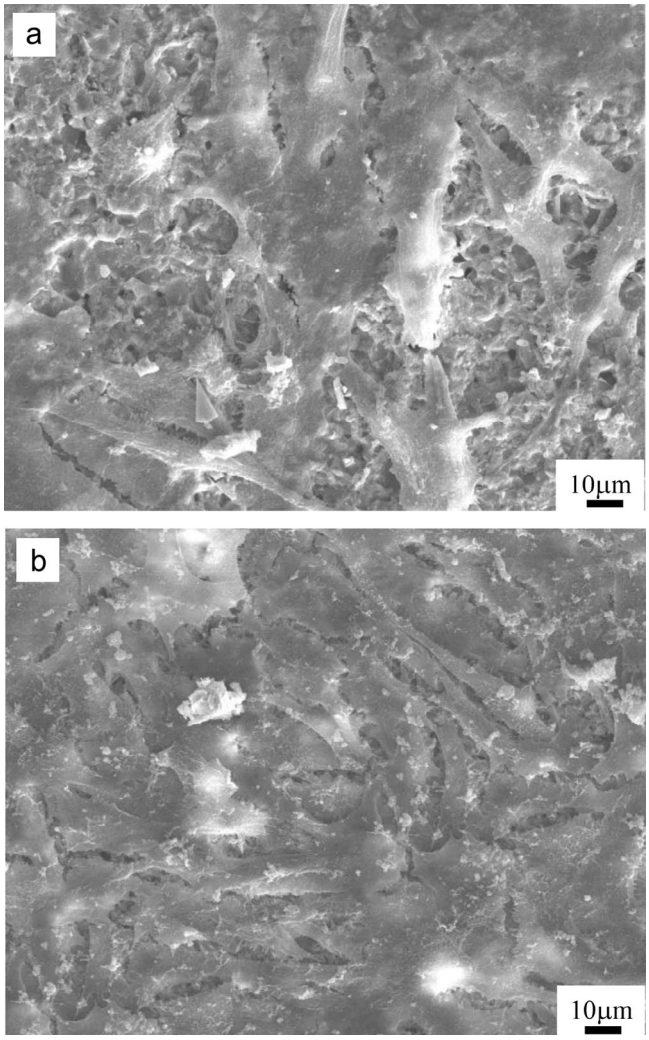

Fig. 8: SEM images of MG63 cells cultured on the PLLA/HA composites
(a) 3 days
(b) 7 days.

IV. Conclusions

Novel PLLA/HA composites with different HA content were prepared with the co-precipitation, tape casting and lamination method. In the composites obtained, a high bending strength of 77.7 MPa was obtained at 50 wt% HA. The elastic modulus increased constantly with the increase

in HA content, while the strain to failure decreased with the addition of HA. The fracture surface of PLLA/HA samples showed a pull-out of HA nanorods. The obtained PLLA/HA composites with satisfactory properties may find application in orthopedic surgery.

Acknowledgements

This work was supported by the National Natural Science Foundation of China (No. 50772128), the Shanghai Science and Technology Committee (No. 07DJ14001, No.07pj14094), and the State Key Laboratory of High Performance Ceramics and Superfine Microstructures. The authors are grateful to Prof. Xuanyong Liu for help with the cell test.

References

1 de Groot, K.: Effect of porosity and physicochemical properties on the stability, resorption, and strength of calcium phosphate ceramics, *Ann. N. Y. Acad. Sci.*, **523**, 227-233, (1988).

2 Weiner, S., Wagner, H.D.: THE MATERIAL BONE: Structure-Mechanical Function Relations, *Annu. Rev. Mater. Sci.*, **28**, 271-298, (1998).

3 Chang, M.C., Ko, C.C., Douglas, W.H.: Conformational change of hydroxyapatite/gelatin nanocomposite by glutaraldehyde, *Biomaterials*, **24**, 3087-3094, (2003).

4 Yaylaoğlu, M.B., Korkusuz, P., Örs, Ü., Korkusuz, F., Hasirci, V.: Development of a calcium phosphate-gelatin composite as a bone substitute and its use in drug release, *Biomaterials*, **20**, 711-719, (1999).

5 Bradt, J.H., Mertig, M., Teresiak, A., Pompe, W.: Biomimetic mineralization of collagen by combined fibril assembly and calcium phosphate formation, *Chem. Mater.,* **11**, 2694-2701, (1999).

6 Miyaji, F., Kim, H.M., Handa, S., Kokubo, T., Nakamura, T.: Bonelike apatite coating on organic polymers: novel nucleation process using sodium silicate solution, *Biomaterials*, **20**, 913-919, (1999).

7 Ignjatović, N., Tomić, S., Dakić, M., Miljković, M., Plavsić, M., Uskoković, D.: Synthesis and properties of hydroxyapatite/poly-L-lactide composite biomaterials, *Biomaterials,* **20**, 809-816, (1999).

8 Bigi, A., Boanini, E., Panzavolta, S., Roveri, N.: Biomimetic growth of hydroxyapatite on gelatin films doped with sodium polyacrylate, *Biomacromolecules,* **1**, 752-756, (2000).

9 Shanmugasundarm, N., Ravichandran, P., Peddy, P.N., Ramamurty, N., Pal, S., Rao, K.P.: Collagen-chitosan polymeric scaffolds for the in-vitro culture of human epidermoid carcinoma cells, *Biomaterials*, **22**,1943-1951, (2001).

10 Zhao, F., Yin, Y.J., Lu, W.W., Leong, J.C., Zhang, W.Y., Zhang, J.Y., Zhang, M.F., Yao, K.D.: Preparation and histological evaluation of biomimetic three-dimensional hydroxyapatite/chitosan-gelatin network composite scaffolds, *Biomaterials*, **23**, 3227-3234, (2002).

11 Yin, Y.J., Ye, F., Cui, J.F., Zhang, F.J., Li, X.L., Yao, K.D.: Preparation and characterization of macroporous chitosan-gelatin beta-tricalcium phosphate composite scaffolds for bone tissue engineering, *J. Biomed. Mater. Res.*, **A 67**, 844-855, (2003).

12 Hartgerink, J.D., Beniash, E., Stupp, S.I.: Self-assembly and mineralization of peptide-amphiphile nanofibers, *Science*, **294**, 1684-1688, (2001).

13 Kikuchi, M., Itoh, S., Ichinose, S., Shinomiya, K., Tanaka, J.: Self-organization mechanism in a bone-like hydroxyapatite/collagen nanocomposite synthesized in vitro and its biological reaction in vivo, *Biomaterials,* **22**, 1705-1711, (2001).

14 Yang, Y., Magnay, J.L., Cooling L., El Haj, A.J.: Development of a 'mechano-active' scaffold for tissue engineering, *Biomaterials* ,**23**, 2119-2126, (2002).

15 Park, S.N., Park, J.C., Kim, H.O., Song, M.J., Suh, H.: Characterization of porous collagen/hyaluronic acid scaffold modified by 1-ethyl-3-(3-dimethylaminopropyl)carbodiimide cross-linking, *Biomaterials*, **23**, 1205-1212, (2002).

16 Zhang, W., Liao S.S., Cui, F.Z.: Hierarchical self-assembly of nano-fibrils in mineralized collagen, *Chem. Mater.,* **15**, 3221-3226, (2003).

17 Zhao, B., Hu, H., Mandal S.K., Haddon, R.C.: A bone mimic based on the self-assembly of hydroxyapatite on chemically functionalized single-walled carbon nanotubes, *Chem. Mater.,* **17**, 3235-3241, (2005).

18 Descalzo, A.B., Martínez-Máñez, R., Sancenón, F., Hoffmann, K., Rurack, K.: The Supramolecular Chemistry of Organic-Inorganic Hybrid Materials, *Angew. Chem. Int. Edn.*, **45**, 5924-5948, (2006).

19 Stupp, S.I., Braun, P.V.: Molecular manipulation of microstructures: Biomaterials, ceramics, and semiconductors, *Science*, **277**, 1242-1248, (1997).

20 Chen, H.F., Clarkson, B.H., Sun, K., Mansfield, J.F.: Self-assembly of synthetic hydroxyapatite nanorods into an enamel prism-like structure, *J.Colloid. Interface Sci.,* **288**, 97-103, (2005).

21 Chen, J.D., Wang, Y.J., Wei, K., Zhang, S.H., Shi, X.T.: Self-organization of hydroxyapatite nanorods through oriented attachment, *Biomaterials*, **28**, 2275-2280, (2007).

22 Ye, F., Guo, H.F., Zhang, H.J., Biomimetic synthesis hydroxyapatite mediated surfactants, *Nanotechnology*, **19**, 245605, (2008).

23 Vainionpää, S., Rokkanen, P., Törmälä, P.: Surgical applications of biodegradable polymers in human tissues, *Prog. Polym. Sci.*, **14**, 679-716, (1989).

24 Edlund, U., Albertsson, A.C.: Degradable polymer microspheres for controlled drug delivery, *Adv. Polym. Sci.*, **157**, 67-112, (2002).

25 Sarazin, P., Roy, X., Favis, B.D.: Controlled preparation and properties of porous poly (L-lactide) obtained from a co-continuous blend of two biodegradable polymers, *Biomaterials*, **25**, 5965-5978, (2004).

26 Ylinen, P.: Filling of bone defects with porous hydroxyapatite reinforced with polylactide or polyglycolide fibers, *J. Mater. Sci. Mater. Med.*, **5**, 522-528, (1994).

27 Hofmann, G.O.: Biodegradable implants in traumatology – a review on the state-of-the-art, *Arch. Orthop. Trauma. Surg.*, **114**, 123-32, (1995).

28 Bostman, O.M.: Metallic or absorbable fracture fixation devices. A cost minimization analysis, *Clin. Orthop. Relat. Res.*, **329**, 233-239, (1996).

29 Leclerc, E., Furukawa, K.S., Miyata, F., Sakai, Y., Ushida, T., Fujii, T.: Fabrication of microstructures in photosensitive biodegradable polymers for tissue engineering applications, *Biomaterials*, **25**, 4683-4690, (2004).

30 Leiggener, C.S., Curtis, R., Muler, A.A., Pfluger, D., Gogolewski, S., Rahn, B.A.: Influence of copolymer composition of polylactide implants on cranial bone regeneration, *Biomaterials*, **27**, 202-207, (2006).

31 Osther, P.J., Gjode, P., Mortensen, B.B., Bartholin, J., Gottrup, F.: Randomized comparison of polyglycolic acid and polyglyconate sutures for abdominal fascial closure after laparotomy in patients with suspected impaired wound healing, *Br. J. Surg.*, **82**, 1080-1082, (1995).

32 Aguilar, C.A., Lu, Y., Mao, S., Chen, S.C.: Direct micro-patterning of biodegradable polymers using ultraviolet and femtosecond lasers, *Biomaterials*, **26**, 7642-7649, (2005).

[33] Wood, J.S., Frost, D.B.: Results using the biofragmentable anastomotic ring for colon anastomosis, *Am. Surg.*, **59**, 642-644, (1993).

[34] Verheyen, C.C.P.M., de Wijn, J.R.., van Blitterswijk, C.A., de Groot, K., Rozing, P.M.: Hydroxylapatite/poly(L-lactide) composites: an animal study on push-out strengths and interface histology, *J. Biomed. Mater. Res.*, **27**, 433-444, (1993).

[35] Yasunaga, T., Matsusue, Y., Furukawa, T., Shikinami, Y., Okuno, M., Nakamura, T.: Bonding behaviour of ultrahigh strength unsintered hydroxyapatite particles/poly(L-lactide) composites to surface of tibial cortex in rabbits, *J. Biomed. Mater. Res.*, **47**, 412-419, (1999).

[36] Wang, G.C., Meng, F.H., Ding, C.X., Chu, P.K., Liu, X.Y: Microstructure, bioactivity and osteoblast behavior of monoclinic zirconia coating with nanostructured surface, *Acta Biomaterialia*, **6**, 990-1000, (2010).

[37] Landi, E., Tampieri, A., Celotti, G., Sprio, S.: Densification behaviour and mechanisms of synthetic hydroxyapatites, *J. Eur. Ceram. Soc.*, **20**, 2377-2387, (2000).

[38] Rodríguez-Lorenzo, L.M., Vallet-Regí, M.: Controlled Crystallization of Calcium Phosphate Apatites, *Chem. Mater.,* **12**, 2460-2465, (2000).

[39] Kasuga, T., Ota, Y., Nogami, M., Abe, Y.: Preparation and mechanical properties of polylactic acid composites containing hydroxyapatite fibres, *Biomaterials*, **22**, 19-23, (2001).